



Quantitative Assessment of CMTM6 in the Tumor Microenvironment and Association with Response to PD-1 Pathway Blockade in Advanced-Stage Non-Small Cell Lung Cancer

Jon Zugazagoitia, MD, PhD,^a Yuting Liu, BS,^a Maria Toki, MD,^{a,b} John McGuire, BS,^a Fahad Shabbir Ahmed, MD,^a Brian S. Henick, MD,^c Richa Gupta,^a Scott N. Gettinger, MD,^d Roy S. Herbst, MD, PhD,^d Kurt A. Schalper, MD, PhD,^{a,d} David L. Rimm, MD, PhD^{a,d,*}

^aDepartment of Pathology, Yale University School of Medicine, New Haven, Connecticut

^bDepartment of Medicine, Sotiria General Hospital, Athens School of Medicine, Athens, Greece

^cDepartment of Medicine (Oncology), Columbia University Medical Center, New York, New York

^dDepartment of Medicine (Oncology), Yale University School of Medicine, New Haven, Connecticut

Received 3 May 2019; revised 12 August 2019; accepted 12 September 2019
Available online - 9 October 2019

ABSTRACT

Introduction: CKLF like MARVEL transmembrane domain containing 6 (CMTM6) has been described as a programmed death ligand 1 (PD-L1) regulator at the protein level by modulating stability through ubiquitination. In this study, we describe the patterns of CMTM6 expression and assess its association with response to programmed cell death 1 pathway blockade in NSCLC.

Methods: We used multiplexed quantitative immunofluorescence to determine the expression of CMTM6 and PD-L1 in 438 NSCLCs represented in tissue microarrays, including in two independent retrospective cohorts of immunotherapy-treated (n = 69) and non-immunotherapy-treated (n = 258) patients and a third collection of *EGFR*- and *KRAS*-genotyped tumors (n = 111).

Results: Tumor and stromal CMTM6 expression was detected in approximately 70% of NSCLCs. CMTM6 expression was not associated with clinical features or *EGFR/KRAS* mutational status and showed a modest correlation with T-cell infiltration ($R^2 < 0.40$). We found a significant correlation between CMTM6 and PD-L1, which was higher in the stroma ($R^2 = 0.51$) than in tumor cells ($R^2 = 0.35$). In our retrospective NSCLC cohort, neither CMTM6 nor PD-L1 expression alone significantly predicted immunotherapy outcomes. However, high CMTM6 and PD-L1 coexpression in the stromal and CD68 compartments (adjusted hazard ratio = 0.38, $p = 0.03$), but not in tumor cells ($p = 0.15$), was significantly associated with longer overall survival in treated patients but was not observed in the absence of immunotherapy.

Conclusion: This study supports the mechanistic role for CMTM6 in stabilization of PD-L1 in patient tumors and suggests that high coexpression of CMTM6 and PD-L1, particularly in stromal immune cells (macrophages), might identify the greatest benefit from programmed cell death 1 axis blockade in NSCLC.

*Corresponding author.

Disclosure: Dr. Zugazagoitia has received consulting honoraria from Guardant Health. Dr. Herbst has served as a consultant for AbbVie Pharmaceuticals, AstraZeneca, Biodesix, Bristol-Myers Squibb, Eli Lilly and Company, EMD Serrano, Genentech/Roche, Heat Biologics, Loxo Oncology, Merck and Company, Nektar, NextCure, Novartis, Pfizer, Sanofi, Seattle Genetics, Shire PLC, Spectrum Pharmaceuticals, Symphogen, and Tesaro, and he has received research support from AstraZeneca, Eli Lilly and Company, and Merck and Company. Dr. Schalper has served as a consultant and adviser or served on a scientific advisory board for Celgene, Moderna Therapeutics, and Shattuck Labs, and he has received research funding from Genoptix/Navigate (Novartis), Vasculox/Tioma, Tesaro, Onkaido Therapeutics, Pharmaceuticals, Surface Oncology, Pierre-Fabre Research Institute, Merck, and Bristol-Myers Squibb. Dr. Rimm has served as a consultant and adviser or served on a scientific advisory board for Amgen, AstraZeneca, Agendia, Biocept, BMS, Cell Signaling Technology, Cepheid, Daiichi Sankyo, GSK, Merck, NanoString, Perkin Elmer, PAIGE, and Ultivue, and he has received research funding from AstraZeneca, Cepheid, Navigate/Novartis, NextCure, Lilly, Ultivue, and Perkin Elmer. The remaining authors declare no conflict of interest.

Address for correspondence: David L. Rimm, MD, PhD, Yale Pathology Tissue Services, Department of Pathology, BML 116, Yale University School of Medicine, 310 Cedar St., PO Box 208023, New Haven, CT 06520-8023. E-mail: david.rimm@yale.edu

© 2019 International Association for the Study of Lung Cancer. Published by Elsevier Inc. All rights reserved.

ISSN: 1556-0864

<https://doi.org/10.1016/j.jtho.2019.09.014>

© 2019 International Association for the Study of Lung Cancer. Published by Elsevier Inc. All rights reserved.

Keywords: CMTM6; PD-L1; Macrophages; Immune checkpoint blockade; NSCLC

Introduction

Monoclonal antibodies targeting the programmed cell death 1 (PD-1) pathway have transformed the treatment landscape of advanced-stage NSCLC. However, despite substantial improvements in overall survival (OS), only a minority of patients ($\approx 20\%$) truly benefit from these drugs when given as monotherapies.¹ Programmed death ligand 1 (PD-L1) expression assessed by immunohistochemistry is the most widely used biomarker in the clinic, but it has only modest predictive performance. In NSCLC, although the benefit from PD-1 axis blockade is largely restricted to patients with PD-L1-expressing tumors, some PD-L1-negative NSCLCs respond to these drugs ($\approx 8\%$),²⁻⁴ and the response rates in those patients most likely to benefit (PD-L1 tumor proportion score $\geq 50\%$) are around 45%.⁵ Given that the benefit from PD-1 pathway blockade in patients with NSCLC is higher in the presence of high PD-L1,⁶ we hypothesized that the study of regulatory pathways involved in PD-L1 expression, rather than PD-L1 alone, could be a way to improve the ability to predict outcomes to these agents.

Chemokine-like factor (CKLF)-like MARVEL transmembrane domain containing family member 6 (CMTM6) has recently been identified as one of the main PD-L1 regulators in two large-scale genetic screens.^{7,8} Mechanistically, both groups independently demonstrated that CMTM6 interacts with PD-L1 in the plasma membrane and recycling endosomes, preventing its lysosomal degradation.^{7,8} CMTM6 appears to function by inhibition of ubiquitination and, thus, stabilization of PD-L1 in the membrane. CMTM6 depletion led to a robust decrease in constitutive and interferon gamma (IFN- γ)-induced PD-L1 protein levels in cancer cell lines, dendritic cells, and xenografts derived from patients with melanoma, without affecting PD-L1 mRNA levels.⁷ CMTM6 was also shown to induce T-cell suppression by promoting a stable PD-L1 surface expression in the plasma membrane.^{7,8}

Despite these mechanistic associations, the distribution and patterns of CMTM6 protein expression, as well as the occurrence of CMTM6 and PD-L1 colocalization in human cancer tissue, have not been comprehensively assessed in patients with lung cancer. In this study, we performed simultaneous measurement of CMTM6 and PD-L1 protein levels in the tumor microenvironment in three independent cohorts of human NSCLC by using

multiplexed quantitative immunofluorescence (QIF). Our primary objective was to address CMTM6 expression, alone or coexpressed with PD-L1, as a potential predictive biomarker to PD-1 pathway blockade in NSCLC.

Methods

Patient Cohorts and TMA Construction

We analyzed retrospectively collected, formalin-fixed, paraffin-embedded tumor specimens represented in tissue microarray (TMA) format from three independent NSCLC cohorts from Yale. All tissue samples were collected and used with specific consent or waiver of consent under the approval from the Yale Human Investigation Committee (protocol 9505008219). Cohort 1 (YTMA250) contained 288 tumors resected between 2004 and 2011 from patients who never received immune checkpoint inhibitors during their follow-up period⁹; cohort 2 (YTMA310) included 138 tumors resected between 2011 and 2013 with known *EGFR* and *KRAS* genotypes, but without any further clinical annotation¹⁰; and cohort 3 (YTMA404) contained 81 tumors resected between 2010 and 2016 from patients who received PD-1 pathway inhibitors for advanced disease ([Supplementary Table 1](#)). Thus, we used the cohort YTMA404 to assess for biomarkers' predictive performance, whereas the cohort YTMA250 was used to test for prognostic significance of biomarkers of interest. [Table 1](#) summarizes the baseline characteristics of the patients included in the YTMA404 and YTMA250 cohorts. The number of cases in which target proteins were quantified differs from the total number of cases included in each TMA on account of loss of histospots during TMA construction or exclusion of cases after visual inspection for quality control.

Multiplexed Immunofluorescence Staining Protocol

Briefly, after the TMA sections were deparaffinized, we subjected them to antigen retrieval with ethylenediaminetetraacetic acid buffer (pH 8) at 97°C for 20 minutes in a pressure heating container (PT module, Lab Vision). Next, we incubated the slides with a solution of 0.3% hydrogen peroxide in methanol to inactivate endogenous peroxidase for 30 minutes, followed by another 30 minutes of incubation with 0.3% bovine serum albumin with 0.05% Tween-20 blocking solution. Subsequently, we performed a sequential multiplexed immunofluorescence staining (panel 1) with primary antibodies to detect epithelial tumor cells (pan-cytokeratin, polyclonal, Agilent), macrophages (CD68, clone PG-M1, Agilent), CMTM6 (clone RCT6, Absea), and PD-L1 (clone E1L3N, Cell Signaling

Table 1. Baseline Characteristics of the Patients in Cohort 1 and Cohort 3

Characteristic	Immunotherapy-Treated Cohort (YTMA404)		Non-Immunotherapy-Treated Cohort (YTMA250)
	All Patients	Monotherapy and Pretreatment Specimens	
Total quantified tumors, n	69	56	258
Type of immunotherapy			
Single-agent anti-PD-1/PD-L1	58 (84)	56 (100)	
Anti-PD-1/PD-L1 plus anti-CTLA4	9 (13)	0	
Chemotherapy plus anti-PD-1/PD-L1	1 (1)	0	
Other combinations	1 (1)	0	
Specimen type for biomarker assessment, n (%)			
Preimmunotherapy	62 (90)	56 (100)	
Postimmunotherapy	7 (10)	0	
Sex, n (%)			
Male	38 (55)	30 (54)	106 (41)
Female	31 (45)	26 (46)	131 (51)
^a Missing			21
Age, n (%)			
<70 y	35 (51)	25 (45)	132 (51)
≥70 y	34 (49)	31 (55)	104 (40)
^a Missing			22
ECOG performance status, n (%)			
0	6 (9)	5 (9)	
1	54 (79)	43 (77)	
2	8 (12)	7 (12)	
3	1 (1)	1 (2)	
Smoking history, n (%)			
Never-smoker	13 (19)	10 (18)	38 (15)
Current smoker	16 (23)	12 (21)	62 (24)
Former smoker	39 (56)	33 (59)	121 (47)
^a Missing	1	1	37
Histologic type, n (%)			
Adenocarcinoma	50 (72)	41 (73)	135 (52)
Squamous cell carcinoma	15 (22)	12 (21)	63 (24)
Large cell carcinoma	3 (4)	3 (5)	12 (5)
Other	1 (1)		24 (9)
^a Missing			24
Stage, n (%)			
I			147 (57)
II			45 (17)
III	2 (3)	2 (4)	30 (11)
IV (M1a)	18 (26)	15 (27)	10 (4)
IV (M1b)	10 (14)	9 (16)	
IV (M1c)	39 (57)	30 (54)	
^a Missing			26
EGFR mutation status, n (%)			
Wild type	44 (64)	37 (66)	
Mutant	9 (13)	6 (11)	
^a Missing	16	13	
KRAS mutation status, n (%)			
Wild type	32 (46)	25 (45)	
Mutant	18 (23)	15 (27)	
^a Missing	19	16	
CNS metastasis, n (%)			
No	50 (73)	42 (75)	
Yes	18 (26)	13 (23)	
^a Missing	1	1	

(continued)

Table 1. Continued

Characteristic	Immunotherapy-Treated Cohort (YTMA404)		Non-Immunotherapy-Treated Cohort (YTMA250)
	All Patients	Monotherapy and Pretreatment Specimens	
Liver metastasis, n (%)			
No	56 (81)	45 (80)	
Yes	12 (17)	10 (18)	
^a Missing	1	1	
LPI score, n (%)			
Good	28 (41)	22 (39)	
Intermediate	26 (38)	20 (36)	
Poor	4 (6)	4 (7)	
^a Missing	11	10	
Prior therapies, n (%)	15 (22)	9 (16)	
0	34 (49)	30 (54)	
1	19 (27)	16 (28)	
> 1	1	1	

PD-1, programmed cell death 1; PD-L1, programmed death ligand 1; CTLA4, cytotoxic T-lymphocyte associated protein 4; ECOG, Eastern Cooperative Oncology Group; CNS, central nervous system; LPI, Lung Immune Prognostic Index.

^aData not present in clinical chart.

Technology) in the same tissue section. Isotype-specific horseradish peroxidase (HRP)-conjugated secondary antibodies and tyramide-based amplification systems were used for signal detection. Residual HRP activity between sequential secondary antibody incubations was eliminated by exposing the slides twice for 7 minutes to a solution containing 100 mmol/L benzoic hydrazide and 50 mmol/L hydrogen peroxide. We used 4',6-diamino-2-phenylindole (DAPI) to highlight all nuclei. Control slides from a NSCLC titer array (YTMA295) were included in each staining experiment to ensure reproducibility.

To analyze the association between CMTM6 expression and tumor-infiltrating lymphocytes (TILs), we performed a previously standardized multiplexed immunofluorescence TIL staining protocol¹¹ (panel 2) in serial tissue sections from the YTMA404 cohort. Briefly, after tissue sections were subjected to the aforementioned deparaffinization, antigen retrieval, and blocking protocol, we applied primary antibodies to detect epithelial tumor cells (cytokeratin, clone Z0622, Agilent), helper T cells (CD4, clone SP35, Spring Bioscience), cytotoxic T cells (CD8, clone C8/144B, Agilent), and B cells (CD20, clone L26, Agilent) by using a similar sequential protocol with isotype-specific HRP-conjugated secondary antibodies and tyramide-based amplification systems as already described. Control slides from morphologically normal human tonsil were included in each staining batch as positive controls and to ensure reproducibility.

Further details regarding incubation times, antibody clones and concentrations, and fluorescent reagents used can be found in [Supplementary Tables 2 and 3](#).

Fluorescence Signal Quantification and Cutpoint Selection

We used the Automated Quantitative Analysis (AQUA) method (Navigate Biopharma), to quantify the fluorescence signal of CMTM6, PD-L1, and TILs as previously described.¹² CMTM6 and PD-L1 were measured within three compartments: (1) the tumor compartment, created by binarizing the cytokeratin signal; (2) the stromal compartment, created by excluding the tumor mask (a dilated cytokeratin compartment) from a dilated DAPI mask representing the total tissue; and (3) the CD68-positive macrophage compartment, created by binarizing the CD68 signal. A representative image showing these three tissue compartments generated with the AQUA software can be found in [Supplementary Figure 1](#). TILs were measured in the DAPI mask, which was created by dilating and then binarizing the DAPI signal to generate a compartment that included all cells in the histospot. QIF scores were calculated by dividing the target pixel intensity by the area of the compartment of interest (see [Supplementary Fig. 1](#)) and then normalized to the exposure time and bit depth at which the images were captured. Those cases with staining artifacts or presence of less than 2% compartment area were systematically excluded after visual inspection.

For each cohort, we performed staining and target measurement in two independent TMA blocks, with each block containing one nonadjacent tumor core per patient; the average target QIF scores were calculated for each case. Then, we split tumors into high and low CMTM6/PD-L1 expression by using the median as the cutpoint.

Immunotherapy Efficacy Assessment

We used the Response Evaluation Criteria in Solid Tumors, version 1.1, to retrospectively evaluate treatment response to immune checkpoint blockade. As previously described,¹³ we defined clinical benefit as having experienced partial response or stable disease lasting at least 6 months as best response, whereas nonclinical benefit was defined as primary progressive disease or stable disease lasting less than 6 months. Patients with stable disease who did not progress and were censored before 6 months of follow-up were deemed non-evaluable. OS and progression-free survival (PFS) were calculated from the treatment start date to the date of death or loss of follow-up, or the date of disease progression, death, or loss of follow-up, respectively. For those patients who did not die or progress during the study period, the outcome was considered censored. For the purposes of this study, we focused the assessment for predictive significance on the subgroup of patients with preimmunotherapy specimens who received single-agent PD-1 axis blockade ($n = 56$) (see Table 1). Of these 56 patients, 47 received nivolumab (84%), four received pembrolizumab (7%), and five received atezolizumab (9%).

Statistical Analysis

We used the Pearson correlation coefficient to analyze the linear association between two continuous variables and used the t test or one-way analysis of variance to compare the means between two or more groups respectively. The chi-square test was used to compare proportions. Survival curves were estimated with the Kaplan-Meier product-limit method and compared by using the log-rank test. Hazard ratios for OS were calculated by using the Cox regression model. All hypothesis testing was performed at a two-sided significance level of α equal to 0.05.

Results

Initially, we titrated three different anti-CMTM6 antibodies targeting nonoverlapping epitopes in a NSCLC test array (YTMA295) containing 35 lung tumor cores with presumed variable CMTM6 expression (Supplementary Fig. 2A–C). We observed a specific CMTM6 staining pattern localized largely in the plasma membrane with the three antibodies, and we selected the clone RCT6 (Absea) targeting a C-terminal peptide as the reference for validation (Supplementary Fig. 2D–F). Then, we compared the CMTM6 QIF scores obtained with the clone RCT6 with a polyclonal anti-CMTM6 antibody (ab198284, Abcam) targeting a C-terminal peptide and a second anti-CMTM6 monoclonal antibody (clone KT174, Absea) targeting an N-terminal peptide,

showing a high correlation coefficient with both the polyclonal antibody ($R^2 = 0.71$) and the clone KT174 ($R^2 = 0.81$) (Supplementary Fig. 2G and H). In addition, CMTM6 measurement with the RCT6 clone showed good reproducibility between two independent experiments ($R^2 = 0.82$) (Supplementary Fig. 2I). Thus, the RCT6 clone was considered validated and used for the remainder of the studies in this effort.

First, we evaluated the patterns of CMTM6 expression in human NSCLC. Predominantly membranous or cytoplasmic CMTM6 expression was detected in both tumor cells and stromal cells (Fig. 1A–D). In the quantitative analysis, CMTM6 QIF scores showed a continuous distribution, both in the tumor compartment and in the stromal compartment, with the scores being comparable between the three cohorts (Fig. 1E–G). Visually, tumor CMTM6 positivity was detected in about 70% of NSCLCs. In the stroma, almost all tumors were visually positive for CMTM6 to some degree. There was a tight correlation between the CMTM6 QIF scores in the stromal compartment and in the CD68 compartment (Fig. 1H), suggesting that CD68-positive macrophages are a major immune cell type expressing CMTM6 in the stroma. However, some CD68-negative cells also stained positive for CMTM6 in the stroma (Fig. 1I).

To study the association between CMTM6 expression in the tumor microenvironment with lymphocyte infiltration, we stained near tissue sections of YTMA404 with a multiplexed TIL immunofluorescence panel. There was a moderate to weak correlation between tumor or stromal CMTM6 expression and the presence of CD8 T cells ($R^2 = 0.30$ for tumor and $R^2 = 0.31$ for stromal CMTM6) and CD4 T cells ($R^2 = 0.34$ for tumor and $R^2 = 0.39$ for stromal CMTM6). CMTM6 expression showed no correlation with the presence of B lymphocytes ($R^2 = 0.09$ for tumor and $R^2 = 0.008$ for stromal CMTM6).

We found no significant or consistent association between tumor or stromal CMTM6 expression and clinicopathologic factors (Supplementary Tables 4 and 5). Tumor CMTM6 expression was higher in squamous cell carcinomas in the YTMA250 cohort ($p = 0.02$), but these differences were not significant in the YTMA404 cohort (see Supplementary Table 4). Also, tumor or stromal CMTM6 expression levels were not significantly different across *EGFR*- and *KRAS*-mutant NSCLC subgroups (Supplementary Fig. 3A and B). Similarly, PD-L1 expression levels were not significantly different between these NSCLC genomic subgroups (Supplementary Fig. 3C and D).

CMTM6 expression levels were not significantly different between patients with clinical benefit and those with no clinical benefit to single-agent PD-1 axis blockade in YTMA404 cohort (Supplementary Fig. 4A–C). Objective response rates were numerically higher in

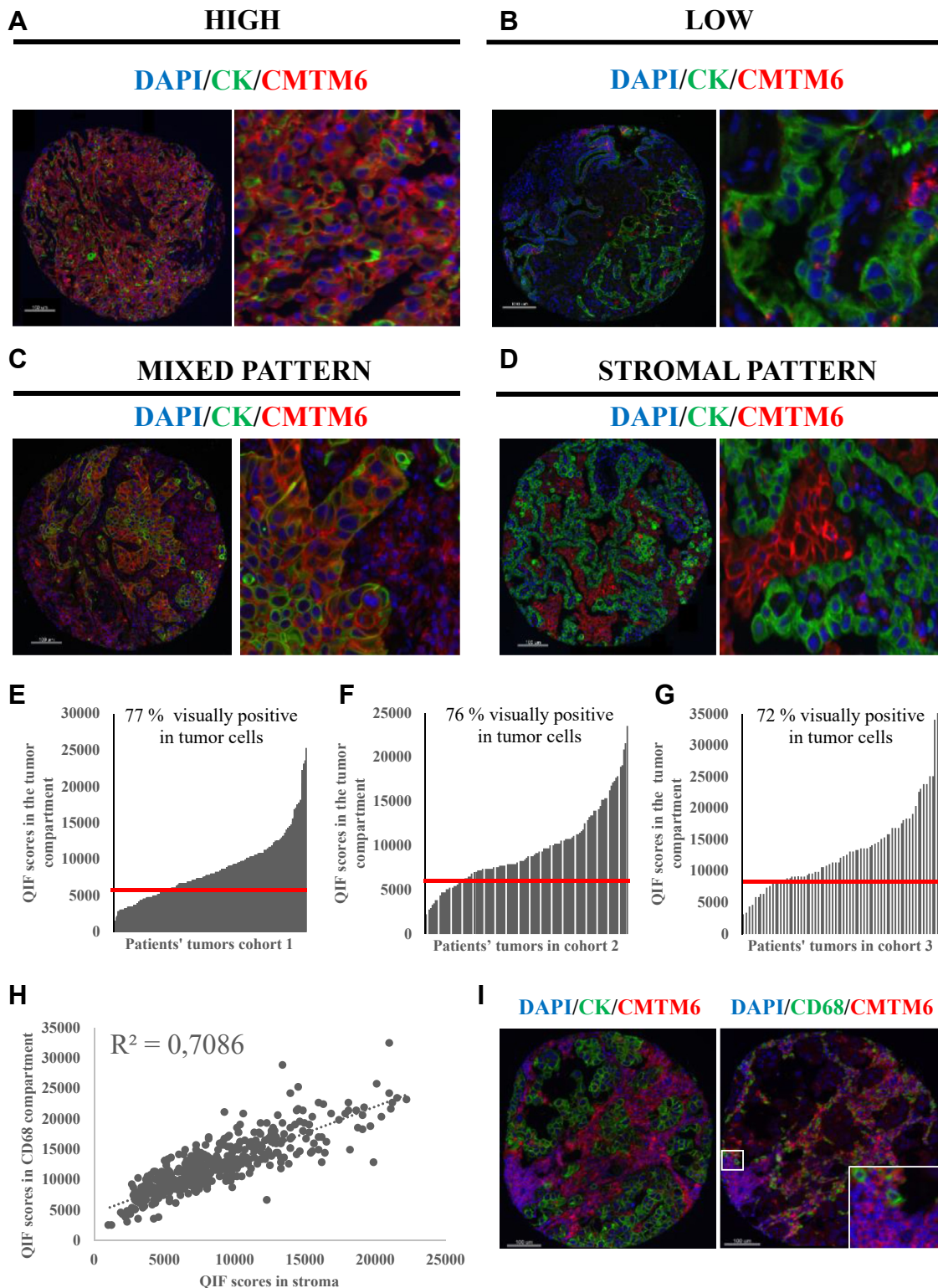


Figure 1. Patterns of expression of CKLF like MARVEL transmembrane domain containing 6 (CMTM6) in human NSCLC tissue. (A and B) Representative cases with high and low CMTM6 expression. (C and D) Representative cases with mixed stromal and tumor CMTM6 expression (C) and stroma-predominant expression (D). (E-G) Dynamic range of CMTM6 expression in the tumor compartment in the three tested cohorts. Red line represents the visual CMTM6 detection threshold in tumor cells. (H) Correlation between CMTM6 quantitative immunofluorescence (QIF) scores in the stromal compartment versus the CD68 molecule (CD68) compartment (three cohorts combined [N = 438]). (I) Representative image of CMTM6 expression in CD68-positive and CD68-negative cells in the stroma. DAPI, 4',6-diamino-2-phenylindole; CK, cytokeratin.

patients with high CMTM6 expression in the stromal (24%) or the CD68 compartments (21.4%) as compared with in those with low CMTM6 expression (6.9% in the stromal compartment and 7.7% in the CD68 compartment), but these differences did not reach statistical significance ($p = 0.07$ and $p = 0.15$, respectively) (Supplementary Table 6). Similarly, CMTM6 expression did not significantly predict PFS (Supplementary Fig. 4D–F) or OS under single-agent PD-1 axis blockade, although those patients with high CMTM6 expression in the stromal and CD68 compartments had a trend toward longer median OS as compared with those with low CMTM6 expression ($p = 0.14$ and $p = 0.13$, respectively) (Fig. 2A–C). In historical control patients who were not treated with immunotherapy, median OS was comparable and not statistically significant between patients with high- and low-CMTM6-expressing tumors in the YTMA250 cohort (Fig. 2D–F).

Next, on the basis of the mechanistic evidence for interaction, we evaluated the association between CMTM6 and PD-L1 expression and their colocalization patterns in human lung cancer tissue. Visually, CMTM6 and PD-L1 colocalized in both tumor cells and immune cells in the stroma (Fig. 3A and B). In the stroma, CMTM6 and PD-L1 colocalization mostly occurred in CD68-positive macrophages (see Fig. 3B). Combining all tumors from the three cohorts ($N = 438$), we found a statistically significant ($p < 0.0001$) but modest correlation between CMTM6 and PD-L1 levels, which were higher in the stromal compartment ($R^2 = 0.51$) and lower in the tumor compartment ($R^2 = 0.35$) (Fig. 3C–D). Notably, all cases with increased PD-L1 showed moderate to high levels of CMTM6, but some cases with increased CMTM6 displayed low or negative PD-L1 expression. This association was similarly observed when the three cohorts were independently analyzed (Supplementary Fig. 5).

Mechanistically, CMTM6 has been shown to stabilize PD-L1 in the cell, which would thus predict that their interaction could indicate PD-L1 function. To test the hypothesis that high CMTM6 and PD-L1 coexpression would exceed the value of either biomarker alone to predict survival benefit from single-agent PD-1 pathway blockade, we first evaluated the predictive performance of PD-L1 expression alone. In this cohort, PD-L1 expression levels in the tumor microenvironment were comparable in patients with clinical benefit and those with no clinical benefit (Supplementary Fig. 6A–C). Objective response rates were significantly higher in patients with high versus low PD-L1 expression in the stromal compartment (26.9% versus 3.9% [$p = 0.016$]) but not in the tumor compartment ($p = 0.44$) (Supplementary Table 7). PFS was not significantly different for patients with high versus low PD-L1

expression in the tumor microenvironment (Supplementary Fig. 6D–F). With regard to OS, PD-L1 expression, measured in the tumor, stromal, or CD68 compartments, and using either the median cutpoint (Fig. 4A–C) or the top 30th percentile (Supplementary Fig. 7), trended toward, but did not significantly predict, longer OS.

Next, we evaluated immunotherapy outcomes in four NSCLC subgroups based on high or low CMTM6 and PD-L1 expression levels (Supplementary Fig. 8). Objective response rates were significantly higher in patients whose tumors showed high CMTM6 and PD-L1 coexpression as compared with the other three phenotypes combined, but only when both were high in the stroma (33.3% versus 3.6% [$p = 0.007$]) or in the CD68 compartment (29.4% versus 8.1% [$p = 0.041$]), and not when coexpressed in the tumor compartment (22.1% versus 11.1% [$p = 0.27$]) (Supplementary Table 8). Median PFS was comparable between the four CMTM6/PD-L1 phenotypes (Supplementary Fig. 9). However, OS was significantly longer in patients whose tumors had high CMTM6 and PD-L1 coexpression as compared the other three expression phenotypes combined, but only when both markers were high in the stromal compartment (23 months versus 6 months [$p = 0.02$]) or CD68 compartments (22 months versus 6 months [$p = 0.03$]), and not in the tumor compartment (22 months versus 12 months [$p = 0.15$]) (Fig. 4C–F). In the multivariable Cox proportional hazard analysis, high CMTM6 and PD-L1 coexpression in the CD68 compartment remained as an independent predictor of OS after adjustment for age, performance status, smoking history, histologic type, Lung Immune Prognostic Index score, and baseline liver metastasis (hazard ratio = 0.38, 95% confidence interval: 0.16–0.92, $p = 0.03$). As an exploratory analysis, we expanded the OS analysis to the full immunotherapy-treated cohort ($n = 69$). Similar to in the monotherapy subgroup, high CMTM6 and PD-L1 coexpression significantly predicted for longer OS in the stromal compartment ($p = 0.005$) and in the CD68 compartment ($p = 0.004$) but not in the tumor compartment ($p = 0.09$), and neither PD-L1 expression alone nor CMTM6 expression alone reached significance for OS prediction (Supplementary Fig. 10).

To be certain that those tumors with the highest levels of expression of both CMTM6 and PD-L1 were truly colocalized, we created a formula for AQUA analysis in the YTMA404 cohort to calculate the percentage of pixels per unit area where the pixels were above the threshold for both CMTM6 and PD-L1 and then divided that value by the number of pixels within the compartment of interest (tumor, stromal, or CD68). The colocalization was significantly higher in the CD68 compartment than in either the tumor or stromal

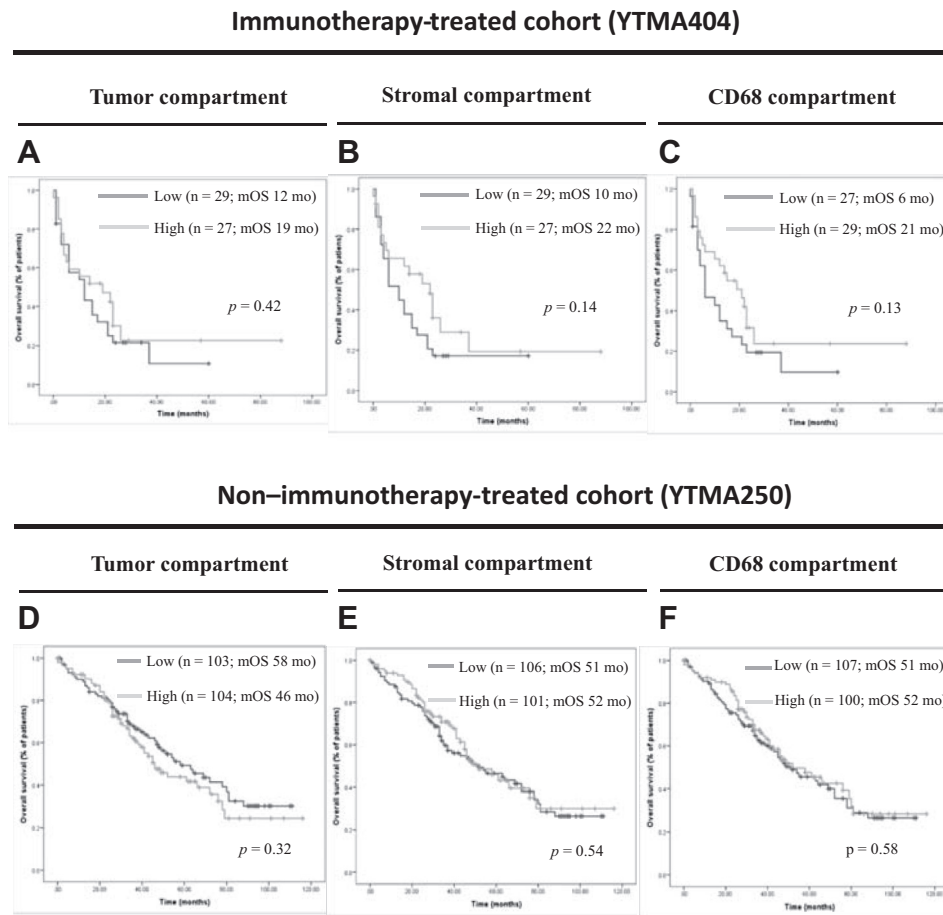


Figure 2. Indicative and prognostic performance of expression of CKLF like MARVEL transmembrane domain containing 6 (CMTM6). (A-C) Overall survival according to CMTM6 expression in the tumor compartment (A), the stromal compartment (B), and the CD68 molecule (CD68) compartment (C) in patients treated with single-agent PD-1 axis blockade. (D-F) Overall survival according to CMTM6 expression in the tumor compartment (D), the stromal compartment (E), and the CD68 compartment in patients not treated with immune therapies. mOS, median overall survival.

compartments (Supplementary Fig. 11). Using this same algorithm, we found that the tumors with high expression of both CMTM6 and PD-L1 were also the tumors that showed a high level of pixel by pixel colocalization independent of compartment (Supplementary Fig. 12).

Finally, we analyzed whether CMTM6 and PD-L1 coexpression had prognostic significance, where we observed that patients with high CMTM6 and PD-L1 coexpression in the tumor microenvironment showed no survival benefit in the absence of immunotherapy (Fig. 4G-I).

Discussion

CMTM6, which was recently described as one of the main positive regulators of PD-L1 expression at the protein level,^{7,8} was found to be up-regulated in most tumor types at the mRNA level,⁷ but little was known regarding protein expression patterns in human cancer tissue. Here, we developed a multiplexed

immunofluorescence panel with primary antibodies to detect epithelial tumor cells, CD68-positive macrophages, PD-L1, and CMTM6 in the same tissue section (panel 1). We decided to target CD68-positive macrophages because a parallel study from our laboratory showed that CD68-positive macrophages are the predominant immune cell type expressing PD-L1.²⁶ We found that CMTM6 was broadly expressed in NSCLC, with most tumors showing both tumor and stromal expression. We showed that CD68-positive macrophages are a major immune cell type expressing CMTM6 in the stroma, but we could not estimate the precise percentage of CD68/CMTM6 double-positive cells in the tumor microenvironment because the AQUA software does not perform cell segmentation and counting.

In this study, we did not attempt to characterize in detail which types of other immune cells express CMTM6, but we did observe that some CD68-negative immune cells were also visually positive for CMTM6.

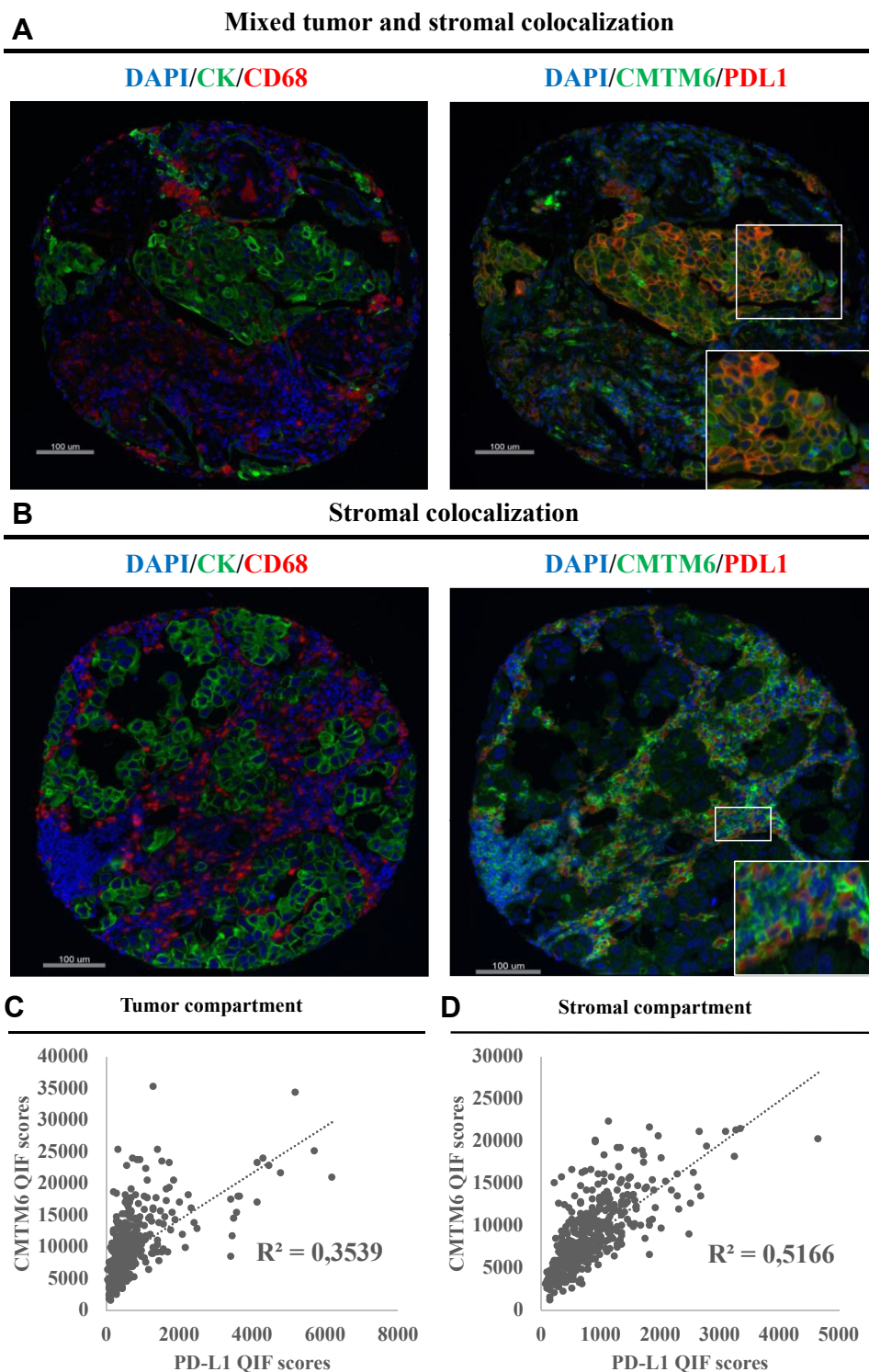
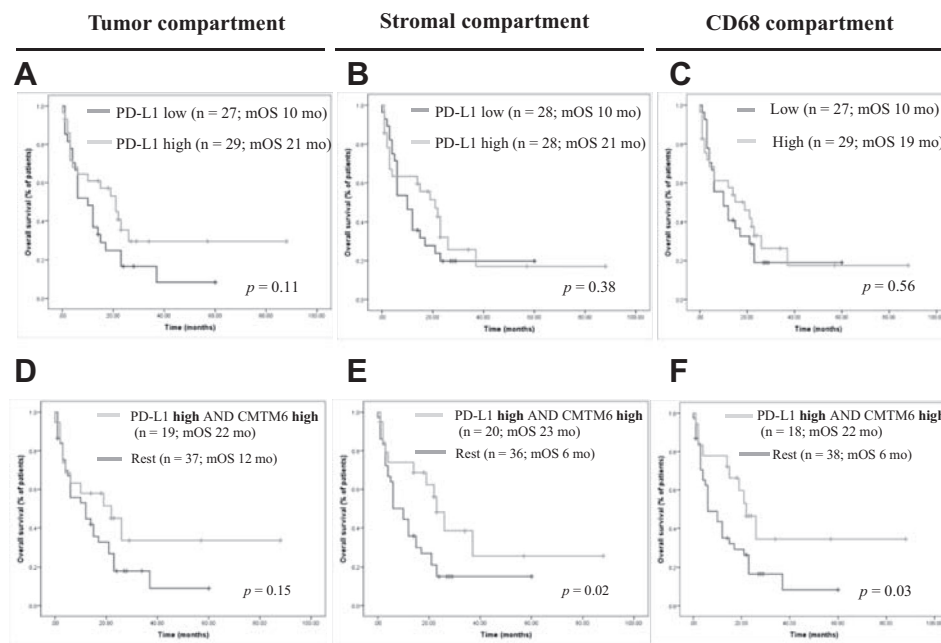


Figure 3. Expression of CKLF like MARVEL transmembrane domain containing 6 (CMTM6) and programmed death ligand 1 (PD-L1) in NSCLC. (A and B) CMTM6 and PD-L1 colocalization in tumor and stroma (A) and stroma only (predominantly in CD68 molecule-positive macrophages) (B). (C and D) Correlation between CMTM6 expression levels and PD-L1 expression levels in the tumor compartment (C) and the stromal compartment (D) ($n = 438$). DAPI, 4',6-diamino-2-phenylindole; CK, cytokeratin; QIF, quantitative immunofluorescence.

On the basis of morphological inspection, most of these cells were probably tumor-associated monocytes and CD68-negative macrophages. We found a modest or

weak correlation between CMTM6 expression and the presence of CD4 and CD8 T cells, but as this multiplexed TIL panel did not include a primary antibody against

Immunotherapy-treated cohort (YTMA404)



Non-immunotherapy-treated cohort (YTMA250)

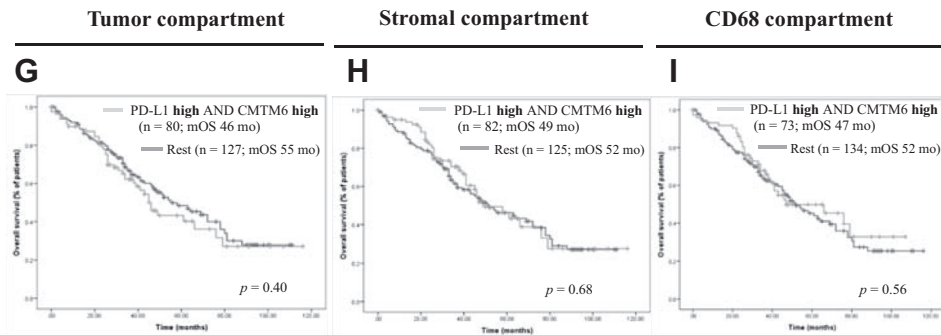


Figure 4. Indicative and prognostic performance of high coexpression of CKLF like MARVEL transmembrane domain containing 6 (CMTM6) and programmed death ligand 1 (PD-L1). (A-C) Overall survival (OS) according to PD-L1 expression alone in the tumor compartment (A), the stromal compartment (B), and the CD68 molecule (CD68) compartment (C) in patients treated with single-agent programmed cell death 1 axis blockade. (D-F) OS in patients with high CMTM6 and PD-L1 coexpression in the tumor compartment (D), the stromal compartment (E), and the CD68 compartment (F) in patients treated with single-agent programmed cell death 1 axis blockade. (G-I) OS in patients with high CMTM6 and PD-L1 coexpression in the tumor compartment (G), the stromal compartment (H), and the CD68 compartment (I) in patients not treated with immunotherapy. mOS, median overall survival.

CMTM6 and was performed in near tissue sections but not in the same tissue section, we could not determine whether T lymphocytes also express CMTM6.

Supporting the findings from previous experimental studies,^{7,8} we found that CMTM6 and PD-L1 colocalize both in tumor cells and CD68-positive macrophages. In the quantitative analysis, the association between both markers was modest but statistically significant, and interestingly, it was higher in the stroma. Notably, cases with increased PD-L1 coexpressed CMTM6, but a

fraction of cases with high CMTM6 displayed low or negative PD-L1 expression, suggesting that CMTM6 upregulation is not sufficient to mediate PD-L1 protein expression in NSCLC. In fact, CMTM6 does not regulate PD-L1 transcriptionally, either in the presence or absence of IFN- γ .^{7,8} Moreover, CMTM6 expression has been shown to be independent of IFN- γ pathway activation.^{8,14} As shown by Burr et al., CMTM6 levels were not influenced by IFN- γ exposure in vitro in several cell line models,⁸ which further supports the existence of

tumors with high levels of CMTM6 but low or undetectable PD-L1. Actually, CMTM6 has likely alternative functions other than PD-L1 binding, which could also explain the imperfect correlation that we observed in tumor tissue. For instance, CMTM6 has been recently found to be involved in lipid and low-density lipid cholesterol uptake by macrophages during atherogenesis.^{15,16} On the other hand, CMTM6 is not the only PD-L1 regulator at the posttranslational level. For example, CMTM4 has been shown to act as a backup PD-L1 protein stabilizer in CMTM6-deficient cells.⁷ Another proposed PD-L1 stabilizer is COP9 signalosome 5 via nuclear factor kappa light-chain enhancer of activated B cells signaling, which inhibits PD-L1 degradation by removing ubiquitin chains.¹⁷ In addition, somatic mutations within the intracytoplasmic domain of PD-L1 in motifs that are targets for ubiquitination and posttranslational modifications have also been shown to affect PD-L1 stability and function,¹⁸ again highlighting the importance of posttranslational modifications in modulating PD-L1-inhibitory functions.

The relationship between CMTM6 expression and outcome is unclear. We found no clear association between CMTM6 expression in the tumor microenvironment with clinical features, genomic features, or outcome in NSCLC. In contrast, previous reports have shown that high CMTM6 expression at the mRNA level was associated with poor prognostic clinical and molecular features in patients with gliomas.^{11,12} In other tumor types, high CMTM6 expression at the RNA level was associated with poor prognosis in pancreatic cancers,¹⁹ but with good prognosis in patients with triple-negative breast cancer.¹⁹ These differences between distinct tumor types might potentially reflect a tissue-specific CMTM6 upregulation or function. To our knowledge, this study is the first report addressing the predictive performance of CMTM6 expression in patients with NSCLC treated with immune checkpoint inhibitors. Although neither CMTM6 expression nor PD-L1 expression alone was significantly associated with better outcomes in patients treated with immunotherapy in this limited-size retrospective cohort, we found that high CMTM6 and PD-L1 coexpression was significantly associated with higher response rates and longer OS under single-agent PD-1 pathway blockade, but interestingly, only when both markers were coexpressed in the stromal and CD68 compartments and not in the tumor compartment. In the absence of prognostic significance in traditionally managed patients, high CMTM6 and PD-L1 coexpression in stromal immune cells (macrophages) might be a novel indicative biomarker to predict benefit from PD-1 axis blockade.

The observation that high CMTM6 and PD-L1 coexpression significantly associates with outcomes

upon PD-1 pathway blockade only in the stroma suggests that the regulatory interaction between CMTM6 and PD-L1 might be biologically more relevant in immune cells than in tumor cells. This finding is consistent with the findings in many of other tumor types where the predictive value of PD-L1 seems to be largely restricted to immune cell expression, such as in urothelial,²⁰ cervical,²¹ head and neck,²² and triple-negative breast cancers.²³ In NSCLC, both tumor cell and immune cell PD-L1 expression have been associated with benefit from PD-1 axis blockade.^{4,24} However, detailed localization studies have not yet been done. Although some studies suggest that PD-L1 in tumor cells is not concordant with PD-L1 expression in immune cells,²⁴ other studies, including one quantitative study, find a tight relationship between tumor cell and immune cell expression of PD-L1.²⁵ If there is a tight correlation between tumor cell and immune cell PD-L1, then the predictive value of response to immune checkpoint inhibition could be uniform for all tumor types. This is also concordant with our recent quantitative study of PD-L1 expression in macrophages.²⁶

This study should be considered in the context of a number of limitations. First, the immunotherapy-treated cohort is a retrospective collection with mixed therapies, not a clinical trial. As such, it is not possible to calculate an interaction score because there is no subset of patients who did not receive immunotherapy. We are able to show absence of prognostic value in a historical cohort and have thus used the term *indicative* rather than the term *predictive*. Furthermore, this study might be underpowered to demonstrate a significant association of PD-L1 expression with survival, as has been the case in some NSCLC clinical trials.^{27,28} Similarly, the small cohort size prevents us from determination of the extent to which the combination of CMTM6 and PD-L1 expression outperforms the established predictive power of PD-L1 expression alone in NSCLC.^{3-5,29} It is also a limitation that we used the median cutpoint to split the population into those with high versus low expression of CMTM6 and PD-L1. Although that point may be near the biologically correct cutpoint, a validation set would be required to optimize the cutpoints. Future studies addressing the predictive value of CMTM6 with or without PD-L1 coexpression will likely require the validation of an optimal and reproducible cutpoint in larger and well-powered cohorts that can be split into training and validation sets. Finally, we used TMAs instead of whole tissue sections for biomarker assessment. As in all good TMA studies, we tried to partially avoid the issue of tumor heterogeneity by staining tumors in a twofold redundancy (two histospots derived from two separate regions of the tumor).

In conclusion, this study supports the mechanistically hypothesized role for CMTM6 in stabilization of PD-L1 in patient tumors in that high levels of coexpression of both CMTM6 and PD-L1 are associated with better outcome in the presence of immune checkpoint inhibitor therapy. Furthermore, coexpression in immune cells, or more specifically macrophages, is consistent with current trends in other tumor types, where immune cells, not tumor cells, are identified as the companion diagnostic test. We believe that this study suggests that extensive further validation of this biomarker may result in a more specific companion diagnostic test for immunotherapy.

Acknowledgments

This work was supported by funds from Navigate BioPharma (Novartis) and Yale Specialized Programs of Research Excellence in Lung Cancer. Dr. Zugazagoitia was supported by a Rio Hortega contract from the Carlos III Research Institute (CM15/00196) and a fellowship from the Spanish Society of Medical Oncology. The authors thank Lori A. Charette and the staff of Yale Pathology tissue services for expert histology services.

Supplementary Data

Note: To access the supplementary material accompanying this article, visit the online version of the *Journal of Thoracic Oncology* at www.jto.org and at <https://doi.org/10.1016/j.jtho.2019.09.014>.

References

1. Gettinger S, Horn L, Jackman D, et al. Five-year follow-up of nivolumab in previously treated advanced non-small-cell lung cancer: results from the CA209-003 study. *J Clin Oncol*. 2018;36:1675-1684.
2. Brahmer J, Reckamp KL, Baas P, et al. Nivolumab versus docetaxel in advanced squamous-cell non-small-cell lung cancer. *N Engl J Med*. 2015;373:123-135.
3. Borghaei H, Paz-Ares L, Horn L, et al. Nivolumab versus docetaxel in advanced nonsquamous non-small-cell lung cancer. *N Engl J Med*. 2015;373:1627-1639.
4. Rittmeyer A, Barlesi F, Waterkamp D, et al. Atezolizumab versus docetaxel in patients with previously treated non-small-cell lung cancer (OAK): a phase 3, open-label, multicentre randomised controlled trial. *Lancet*. 2017;389:255-265.
5. Reck M, Rodriguez-Abreu D, Robinson AG, et al. Pembrolizumab versus chemotherapy for PD-L1-positive non-small-cell lung cancer. *N Engl J Med*. 2016;375:1823-1833.
6. Garon EB, Rizvi NA, Hui R, et al. Pembrolizumab for the treatment of non-small-cell lung cancer. *N Engl J Med*. 2015;372:2018-2028.
7. Mezzadra R, Sun C, Jae LT, et al. Identification of CMTM6 and CMTM4 as PD-L1 protein regulators. *Nature*. 2017;549:106-110.
8. Burr ML, Sparbier CE, Chan Y-C, et al. CMTM6 maintains the expression of PD-L1 and regulates anti-tumour immunity. *Nature*. 2017;549:101-105.
9. Altan M, Pelekanou V, Schalper KA, et al. B7-H3 expression in NSCLC and its association with B7-H4, PD-L1 and tumor-infiltrating lymphocytes. *Clin Cancer Res*. 2017;23:5202-5209.
10. Toki MI, Mani N, Smithy JW, et al. Immune marker profiling and programmed death ligand 1 expression across NSCLC mutations. *J Thorac Oncol*. 2018;13:1884-1896.
11. Brown JR, Wimberly H, Lannin DR, Nixon C, Rimm DL, Bossuyt V. Multiplexed quantitative analysis of CD3, CD8, and CD20 predicts response to neoadjuvant chemotherapy in breast cancer. *Clin Cancer Res*. 2014;20:5995-6005.
12. Camp RL, Chung GG, Rimm DL. Automated subcellular localization and quantification of protein expression in tissue microarrays. *Nat Med*. 2002;8:1323-1327.
13. Rizvi H, Sanchez-Vega F, La K, et al. Molecular determinants of response to anti-programmed cell death (PD)-1 and anti-programmed death-ligand (PD-L)-ligand 1 blockade in patients with non-small-cell lung cancer profiled with targeted next-generation sequencing. *J Clin Oncol*. 2018;36:633-641.
14. Brockmann M, Blomen VA, Nieuwenhuis J, et al. Genetic wiring maps of single-cell protein states reveal an off-switch for GPCR signalling. *Nature*. 2017;546:307-311.
15. Willer CJ, Schmidt EM, Sengupta S, et al. Discovery and refinement of loci associated with lipid levels. *Nat Genet*. 2013;45:1274-1283.
16. Domschke G, Linden F, Pawig L, et al. Systematic RNA-interference in primary human monocyte-derived macrophages: a high-throughput platform to study foam cell formation. *Sci Rep*. 2018;8:10516.
17. Lim S-O, Li C-W, Xia W, et al. Deubiquitination and stabilization of PD-L1 by CSN5. *Cancer Cell*. 2016;30:925-939.
18. Gato-Cañas M, Zuazo M, Arasanz H, et al. PDL1 Signals through conserved sequence motifs to overcome interferon-mediated cytotoxicity. *Cell Rep*. 2017;20:1818-1829.
19. Mamessier E, Birnbaum DJ, Finetti P, Birnbaum D, Bertucci F. CMTM6 stabilizes PD-L1 expression and refines its prognostic value in tumors. *Ann Transl Med*. 2018;6:54.
20. Rosenberg JE, Hoffman-Censits J, Powles T, et al. Atezolizumab in patients with locally advanced and metastatic urothelial carcinoma who have progressed following treatment with platinum-based chemotherapy: a single-arm, multicentre, phase 2 trial. *Lancet*. 2016;387:1909-1920.
21. Chung HC, Schellens JHM, Delord J-P, et al. Pembrolizumab treatment of advanced cervical cancer: updated results from the phase 2 KEYNOTE-158 study. *J Clin Oncol*. 2018;36(suppl 15), 5522-5522.
22. Burtneß B, Harrington KJ, Greil R, et al. LBA8_PRKEY-NOTE-048: phase III study of first-line pembrolizumab (P) for recurrent/metastatic head and neck squamous cell carcinoma (R/M HNSCC). *Ann Oncol*. 2018;29(suppl 8).

23. Schmid P, Adams S, Rugo HS, et al. Atezolizumab and Nab-paclitaxel in advanced triple-negative breast cancer. *N Engl J Med*. 2018;379:2108-2121.
24. Fehrenbacher L, Spira A, Ballinger M, et al. Atezolizumab versus docetaxel for patients with previously treated non-small-cell lung cancer (POPLAR): a multi-centre, open-label, phase 2 randomised controlled trial. *Lancet*. 2016;387:1837-1846.
25. Rehman JA, Han G, Carvajal-Hausdorf DE, et al. Quantitative and pathologist-read comparison of the heterogeneity of programmed death-ligand 1 (PD-L1) expression in non-small cell lung cancer. *Mod Pathol*. 2017;30:340-349.
26. Liu Y, Zugazagoitia J, Ahmed FS, et al. Immune cell PD-L1 co-localizes with macrophages and is associated with outcome in PD-1 pathway blockade therapy. *Clinical Cancer Research*, in press.
27. Carbone DP, Reck M, Paz-Ares L, et al. First-line nivolumab in stage IV or recurrent non-small-cell lung cancer. *N Engl J Med*. 2017;376:2415-2426.
28. Barlesi F, Vansteenkiste J, Spigel D, et al. Avelumab versus docetaxel in patients with platinum-treated advanced non-small-cell lung cancer (JAVELIN Lung 200): an open-label, randomised, phase 3 study. *Lancet Oncol*. 2018;19:1468-1479.
29. Herbst RS, Baas P, Kim D-W, et al. Pembrolizumab versus docetaxel for previously treated, PD-L1-positive, advanced non-small-cell lung cancer (KEYNOTE-010): a randomised controlled trial. *Lancet*. 2016;387:1540-1550.